

Supplementary Material

Raman intensity enhancement of molecules adsorbed on HfS₂ flakes up to 200 layers

Xiao Fei Yue, Yao Liang, Jie Jiang, Rong Gang Liu, Shou Tian Ren, Ren Xi Gao, Bo Zhong, Guang Wu Wen, Ying Ying Wang* and Ming Qiang Zou*

1. Raman integrated intensities of E_g mode and A_{1g} mode in HfS₂ flakes as a function of number of layers

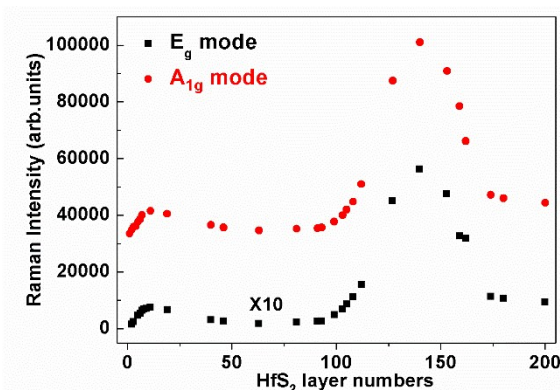


Fig.S1 Raman integrated intensities of E_g mode and A_{1g} mode in HfS₂ flakes as a function of number of layers (NL).

Fig.S1 gives Raman integrated intensities of E_g mode and A_{1g} mode in HfS₂ flakes as a function of number of layers (NL). From this figure, it can be seen, both two modes exhibit the same intensity tendency, indicating the variation of Raman intensities with NL is independent of the lattice vibration modes. Besides, A_{1g} mode is much stronger than E_g mode in intensity. Therefore, the stronger A_{1g} mode is used to study the interference effect in order to reduce the error associated with results from Lorentzian fitting of weak Raman band.

2. Raman integrated intensity of A_{1g} mode in HfS₂ flakes as a function of HfS₂ layer number: the theoretical calculation

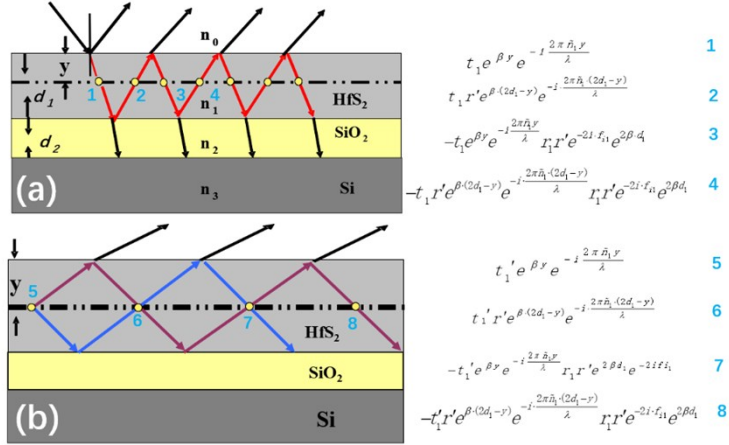


Fig.S2 (a)Schematic laser reflection and transmission in certain depth y in HfS₂ flakes deposited on SiO₂/Si substrate. (b)Multi-reflection of the scattering Raman light from depth y at the interface HfS₂/air and HfS₂/SiO₂ on Si.

The Raman integrated intensity of A_{1g} mode in HfS₂ flakes on SiO₂(300 nm)/Si substrate as a function of NL is calculated based on Fresnel's equations. Consider light incidents from air ($n_0=1$) onto a HfS₂/SiO₂/Si system, as schematically shown in Fig. S2(a). $\tilde{n}_1=3.00-0.06i$, $n_2=1.46$, $\tilde{n}_3=4.15-0.044i$, are refractive indices of HfS₂, SiO₂, and Si at 532 nm, respectively. d_1 is the thickness of HfS₂ which is estimated as $d_1=N \Delta d$, and $\Delta d=0.6$ nm is the thickness of single layer HfS₂, N is the number of layers. d_2 is the thickness of SiO₂ and the Si substrate is considered as semi-infinite.

When a beam of light is incident on an interface, for example, the air/HfS₂ or HfS₂/SiO₂ interface, a portion of the beam is reflected and the rest is transmitted, resulting in an infinite number of transmitted/reflected beams. The Raman intensity of A_{1g} mode in HfS₂ flakes depends on the total electric field distribution, which is a result of interference between all these transmitted beams in HfS₂ flakes.

The total amplitude of incident electric field at certain depth y in HfS₂ flakes is the sum of those infinite transmitted beams in HfS₂ flakes. The amplitudes of first four components of split incident light in HfS₂ flakes (schematically shown in Fig. S2(a)) after considering absorption as well as phase shift are:

$$t_1 e^{\beta y} e^{-i \frac{2\pi \tilde{n}_1 y}{\lambda}},$$

$$t_1 r' e^{\beta(2d_1-y)} e^{-i \frac{2\pi \tilde{n}_1 (2d_1-y)}{\lambda}},$$

$$\begin{aligned}
& -t_1 e^{\beta y} e^{-j \frac{2\pi n_0 y}{\lambda}} r_1 r' e^{-2i \cdot f_{i1}} e^{2\beta \cdot d_1}, \\
& -t_1 r' e^{\beta(2d_1-y)} e^{-j \frac{2\pi n_0(2d_1-y)}{\lambda}} r_1 r' e^{-2i \cdot f_{i1}} e^{2\beta d_1}, \dots
\end{aligned} \tag{1}$$

where $\beta = \frac{-2\pi \cdot k_1}{\lambda}$, (the extinction coefficient of HfS₂ at 532 nm is taken as $k_1 = 0.06$, λ is the excitation wavelength) emerges as a measure of the absorption in HfS₂ layer, $t_1 = \frac{2n_0}{n_0 + \tilde{n}_1}$ is transmission coefficient at the interface of air/HfS₂, $r_1 = \frac{n_0 - \tilde{n}_1}{n_0 + \tilde{n}_1}$ is the reflection coefficient at the air/HfS₂ interface, while $f_{i,2} = \frac{2\pi \cdot \tilde{n}_{1,2} \cdot d_{1,2}}{\lambda}$ are the phase differences when light passes through HfS₂ layers and SiO₂ layers. Here, $r' = \frac{r_2 + r_3 \cdot e^{-2i \cdot f_{i2}}}{1 + r_2 \cdot r_3 \cdot e^{-2i \cdot f_{i2}}}$ is the effective reflection coefficient of HfS₂/(SiO₂ on Si) interface, where $r_2 = \frac{\tilde{n}_1 - n_2}{\tilde{n}_1 + n_2}$, $r_3 = \frac{\tilde{n}_2 - \tilde{n}_3}{\tilde{n}_2 + \tilde{n}_3}$ are reflection coefficients at the interface of HfS₂/SiO₂ and SiO₂/Si, individually.

Thus, the total amplitude of incident electric field at depth y in HfS₂ flakes which is summation of two geometric series can be calculated by:

$$t = \frac{(t_1 e^{\beta y} e^{-j \frac{2\pi n_0 y}{\lambda}} + t_1 r' e^{\beta(2d_1-y)} e^{-j \frac{2\pi n_0(2d_1-y)}{\lambda}}) (1 - (-r_1 r' e^{-2i \cdot f_{i1}} e^{2\beta \cdot d_1})^n)}{1 + r_1 r' e^{-2i \cdot f_{i1}} e^{2\beta \cdot d_1}} \tag{2}$$

Here, $n \rightarrow \infty$ and $-r_1 r' e^{-2i \cdot f_{i1}} e^{2\beta d_1}$ is the common ratio for those two geometric series.

In addition to the above discussion, further consideration should be applied to the interference of multi-reflection of the Raman light in HfS₂ at the interface of HfS₂/air and HfS₂/(SiO₂ on Si), which contribute to the detected Raman signal. Fig. S2(b) shows multi-reflection of the scattering light in certain depth y in HfS₂ flakes and the first four components of scattering light are also schematically shown. Thus, the detected signal is a result of summation of infinite transmitted light from the interface of HfS₂/air, which makes the amplitude multiplied by

$$r = \frac{((e^{\beta y} e^{-j \frac{2\pi n_0 y}{\lambda}} + r' e^{\beta(2d_1-y)} e^{-j \frac{2\pi n_0(2d_1-y)}{\lambda}}) t_1') (1 - (-r_1 r' e^{2\beta d_1} e^{-2i \cdot f_{i1}})^n)}{1 + r_1 r' e^{2\beta d_1} e^{-2i \cdot f_{i1}}} \tag{3}$$

Here, $n \rightarrow \infty$ and $-r_1 r' e^{-2i \cdot f_{i1}} e^{2\beta d_1}$ is the common ratio for two geometric series.

$t'_1 = \frac{1 - r_1^2}{t_1}$ represents the transmission coefficient at the interface of HfS₂/air. The interference, absorption and phase shift of Raman scattering light in HfS₂ flakes are all considered in the calculation.

Thus, the total Raman signal as a result of interference of infinite transmitted laser optical paths in HfS₂ flakes followed by considering the interference of multi-reflection of Raman scattering light can be expressed as:

$$I = \int_0^{d_1} |t \cdot \gamma|^2 dy \quad (4)$$

For R6G molecules adsorbed on HfS₂/SiO₂(300 nm)/Si substrate, the Raman intensities of R6G molecules can be obtained by extending above calculations to a four-layer structure (R6G/HfS₂/SiO₂(300 nm)/Si).

3. The effect of objective NA on Raman intensities of A_{1g} mode in HfS₂ flakes.

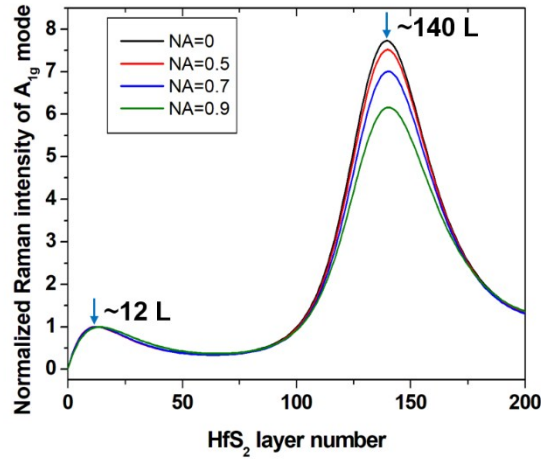


Fig. S3 Calculated integrated Raman intensities of A_{1g} mode in HfS₂ flakes as a function of various NA values of objective lens. The intensity of the first peak has been normalized as 1.

The effect of objective NA on Raman intensities of A_{1g} mode in HfS₂ flakes is calculated by numerical integration of the total Raman signal over the solid angle determined by each NA

$$I = \int_0^{\theta_m} \int_0^{d_1} |t \cdot \gamma|^2 dy W(\theta) d\theta \quad (5)$$

Where $\theta_m = \arcsin(\text{NA})$ and $W(\theta)$ is a weight function which indicates the angular distribution of the collected light, a Gaussian distribution for $W(\theta)$, with $W(\theta) = e^{-\frac{2 \sin^2 \theta}{\sin^2 \sigma}}$

and $\sigma = \theta_m / 3$ is used in this calculation. Fig.S3 shows the Raman intensities of A_{1g} mode in HfS_2 flakes as a function of NA. It also can be seen oblique incidence doesn't cause a large deviation from normal incident. The interference patterns with the first peak at $\sim NL=12$ and the second peak at $\sim NL=140$ are duplicated for different NA. Therefore, normal incident is used in the calculation.

4.Effects of refractive indices on Raman intensities of two-dimensional (2D) materials with different thicknesses deposited on $SiO_2(305\text{ nm})/Si$ substrate

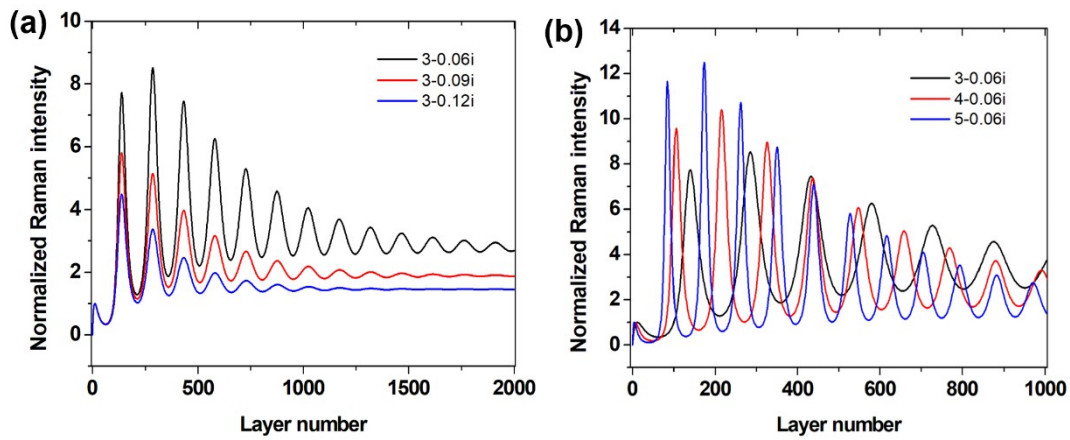


Fig.S4 (a) Normalized Raman intensities of 2D materials with different k values (k is the imaginary part of the refractive index) as a function of layer number. (b) Normalized Raman intensities of 2D materials with different n value (n is the real part of refractive index) as a function of layer number. In those two figures, the intensities of the first peaks have been normalized as 1. 2D materials with different thicknesses are transferred on $SiO_2(305\text{ nm})/Si$ substrate.

Figs.S4 show the normalized Raman intensities of 2D materials with different k (k is the imaginary part of refractive index) and n (n is the real part of refractive index) values as a function of NL. From this figure, it can be seen the number of enhancement peaks is dependent on the absorption of 2D materials. The low absorption (low k value, especially with high n/k ratio) induces abundant enhancement peaks. High-order enhancement peaks are strong in materials with small k and large n (large n will also shift enhancement peak to low NL value). In this calculation, the thickness of 2D materials is taken as 0.6 nm.

5. Raman spectroscopy study of oxidation effect in HfS₂ flakes

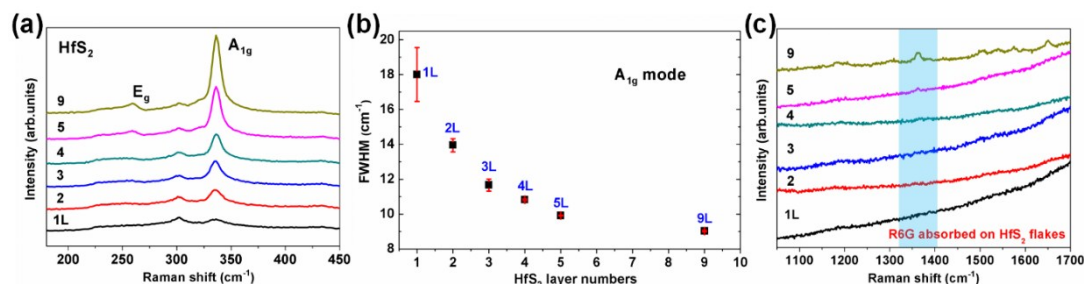


Fig.S5 (a) Raman spectra of HfS₂ flakes with different NL after exposing sample to air for 2 hours. (b) FWHM of A_{1g} mode in HfS₂ flakes. (c) Raman spectra of R6G molecules adsorbed on HfS₂ flakes with different NL. The 1365 cm⁻¹ R6G mode has been highlighted by blue shadow in this figure.

Fig.S5 (a) shows the Raman spectra of HfS₂ flakes with different NL after exposing sample to air for 2 hours. Fig.S5(b) shows Full width at half maximum (FWHM) of A_{1g} mode in HfS₂ flakes with different NL. The FWHM of A_{1g} mode exhibits layer number dependent which is decreasing with increase of layer number. For flake of nine or more layers, the FWHM of A_{1g} mode converge to the bulk value. We attribute the increase in FWHM of A_{1g} mode for a thin HfS₂ flake is due to oxidation are easily happened in a thin HfS₂ flake compared with multi-layer HfS₂. A thin HfS₂ flake is much susceptible to oxygen-rich environment. When expose a thin HfS₂ flake into air, oxidation of a thin HfS₂ flake into a HfO_x film will occur. The phonon life time therefore decreases due to scattering of phonons by defects. The decreased phonon life time induces increasing in FWHM of A_{1g} mode. FWHM of A_{1g} mode therefore can be used as a quantitatively way to identify amounts of defects in HfS₂ flakes. From this result, it also can be seen, multi-layer HfS₂ flakes are much more environmental stable in air.

Further, R6G molecules are adsorbed on HfS₂ flakes with different NL by solution soaking method whose Raman results are given in Fig.S5(c). It can be seen, for a thin HfS₂ flake (< 5 layer), there is no observation of R6G Raman signals. The Raman signal of R6G adsorbed on 5-layer HfS₂ is observed with intensity lower than that on 9-layer HfS₂. We believe this is due to defects are easily formed in a thin HfS₂ flake after exposure to air. With decrease of layer number, more defects are formed in HfS₂ flakes

according to results of FWHM of A_{1g} mode. The oxidation of HfS_2 flakes becomes an obstacle to their Raman enhancements. We also find after longer exposure time, we need thicker HfS_2 flakes to detect the Raman signal of target molecules while thinner flakes have already been oxidized.